Inorganic Chemistry
Article

Inorg. Chem. **2010**, *49*, 9985–9992 **9985**
DOI: 10.1021/ic1012186

Self-Assembled E_2L_3 Cryptands (E = P, As, Sb, Bi): Transmetalation, Homo- and Heterometallic Assemblies, and Conformational Isomerism

Virginia M. Cangelosi, Timothy G. Carter, Justin L. Crossland, Lev N. Zakharov, and Darren W. Johnson*

Department of Chemistry, Materials Science Institute, and the Oregon Nanoscience and Microtechnologies Institute (ONAMI), University of Oregon, Eugene, Oregon 97403-1253, United States

Received June 17, 2010

A series of Group 15-containing homometallic (E_2L_3, E = P, As, Sb, Bi) and heterometallic ($AsSbL_3$, $AsBiL_3$, $PSbL_3$) supramolecular cryptands were prepared by the self-assembly of pnictogen halides with dithiolate ligand or by direct transmetalation from a heavier congener. Structural characterization by single crystal X-ray diffraction shows that the E−S bond distances and S−E−S bond angles are significantly affected by the identity of the pnictogen. ^{1}H NMR spectroscopy reveals that the homometallic cryptands are dynamic in solution: surprisingly one ligand "flips", perturbing the C_3 symmetry of the complex and giving a new asymmetric conformer. Density functional theory calculations were carried out on both the symmetric and the asymmetric conformations of the cryptands, and the energies were compared to those observed by NMR spectroscopy. It was found that the relative stability of the asymmetric cryptand to its symmetric conformer increases with increasing size of the Group 15 element. Finally, it is reported that if two metals are present during the self-assembly process, heterometallic cryptands form. These supramolecular cryptands are reminiscent of their organic analogues, but result from a self-assembly process rather than a stepwise synthesis. Surprisingly, they possess conformational isomerism and exhibit dynamic transmetalation in their reactivity which provides access to otherwise unattainable assemblies.

Introduction

The Group 15 elements range in structure, property, and application as one descends from the non-metals nitrogen and phosphorus (essential to life) to the toxic metalloids arsenic and antimony, to the metal bismuth, the heaviest of all stable elements offering emerging applications in therapeutics and materials science.[1] While they are often overlooked in favor of the transition metals for supramolecular design, the main group elements, Group 15 in particular, can be used to prepare a variety of supramolecular structure types by metal-directed self-assembly.[2−11] When bound by thiolates in the E(III) oxidation state, P, As, Sb, and Bi each have a trigonal pyramidal geometry and a stereochemically active lone pair of electrons. Previously, our group has shown that each of these elements can be positioned interchangeably within self-assembled E_2L_3 cryptands.[12] Here, we expand upon this work by presenting their dynamic solution behavior, "transmetallation" chemistry,

*To whom correspondence should be addressed. E-mail: dwj@uoregon.edu.

(1) Yang, N.; Sun, H. *Coord. Chem. Rev.* **2007**, *251*, 2354–2366.
(2) (a) Pitt, M. A.; Johnson, D. W. *Chem. Soc. Rev.* **2007**, *36*, 1441–1453 and references therein. (b) Carter, T. G.; Vickaryous, W. J.; Cangelosi, V. M.; Johnson, D. W. *Comments Inorg. Chem.* **2007**, *28*, 97–122.
(3) Milios, C. J.; Ioannou, P. V.; Raptopoulou, C. P.; Papaefstathiou, G. S. *Polyhedron* **2009**, *28*, 3199–3202.
(4) Morsali, A.; Masoomi, M. Y. *Coord. Chem. Rev.* **2009**, *253*, 1882–1905.
(5) Santacruz-Juarez, E.; Cruz-Huerta, J.; Hernandez-Ahuactzi, I. F.; Reyes-Martinez, R.; Tlahuext, H.; Morales-Rojas, H.; Hopfl, H. *Inorg. Chem.* **2008**, *47*, 9804–9812.
(6) Cruz-Huerta, J.; Carillo-Morales, M.; Santacruz-Juarez, E.; Hernandez-Ahuactzi, I. F.; Escalante-Garcia, J.; Godoy-Alcantar, C.; Guerrero-Alvarez, J. A.; Hopfl, H.; Morales-Rojas, H.; Sanchez, M. *Inorg. Chem.* **2008**, *47*, 9874–9885.
(7) Hernandez-Ahuactzi, I. F.; Hopfl, H.; Barba, V.; Roman-Bravo, P.; Zamudio-Rivera, L. S.; Beltran, H. I. *Eur. J. Inorg. Chem.* **2008**, 2746–2755.
(8) Kua, J.; Daly, R. C.; Tomlin, K. M.; Duin, A. C. T. v.; Brill, T. B.; Beal, R. W.; Rheingold, A. L. *J. Phys. Chem. A* **2009**, *113*, 11443–11453.
(9) (a) Marcovich, D.; Tapscott, R. E. *J. Am. Chem. Soc.* **1980**, *102*, 5712–5717. (b) Marcovich, D.; Duesler, E. N.; Tapscott, R. E.; Them, T. F. *Inorg. Chem.* **1982**, *21*, 3336–3341.
(10) Biros, S. M.; Yeh, R. M.; Raymond, K. N. *Angew. Chem., Int. Ed.* **2008**, *47*, 6062–6064.
(11) (a) Vickaryous, W. J.; Herges, R.; Johnson, D. W. *Angew. Chem., Int. Ed.* **2004**, *43*, 5831–5833. (b) Vickaryous, W. J.; Healey, E. R.; Berryman, O. B.; Johnson, D. W. *Inorg. Chem.* **2005**, *44*, 9247–9252. (c) Vickaryous, W. J.; Zakharov, L. N.; Johnson, D. W. *Main Group Chem.* **2006**, *5*, 51–59. (d) Cangelosi, V. M.; Sather, A. C.; Zakharov, L. N.; Berryman, O. B.; Johnson, D. W. *Inorg. Chem.* **2007**, *46*, 9278–9284. (e) Cangelosi, V. M.; Zakharov, L. N.; Fontenot, S. A.; Pitt, M. A.; Johnson, D. W. *Dalton Trans.* **2008**, 3447–3453. (f) Pitt, M. A.; Zakharov, L. N.; Vanka, K.; Thompson, W. H.; Laird, B. B.; Johnson, D. W. *Chem. Commun.* **2008**, 3936–3938. (g) Allen, C. A.; Cangelosi, V. M.; Zakharov, L. N.; Johnson, D. W. *Cryst. Growth Des.* **2009**, *9*, 3011–3013. (h) Cangelosi, V. M.; Carter, T. G.; Zakharov, L. N.; Johnson, D. W. *Chem. Commun.* **2009**, 5606–5608. (i) Cangelosi, V. M.; Zakharov, L. N.; Crossland, J. L.; Franklin, B. C.; Johnson, D. W. *Cryst. Growth Des.* **2010**, *10*, 1471–1473. (j) Lindquist, N. R.; Carter, T. G.; Cangelosi, V. M.; Zakharov, L. N.; Johnson, D. W. *Chem. Commun.* **2010**, *46*, 3505–3507.
(12) Cangelosi, V. M.; Zakharov, L. N.; Johnson, D. W. *Angew. Chem., Int. Ed.* **2010**, *49*, 1248–1251.

Published on Web 10/04/2010

and three new examples of chiral, heterometallic $EE'L_3$ cryptands.

Heterometallic assemblies are relatively rare and most are prepared by stepwise synthesis[13] or incorporate ligands with unique binding sites specific for each type of metal based on that metal's preferred coordination number, geometry, charge, hard/soft binding site, or electronic discrimination.[14−23] However, the Group 15 elements within the cryptands reported here are bound by the same coordination sphere of three thiolates revealing a surprising *lack* of selectivity. This series of homo- and heterometallic cryptands allows for the direct comparison of preferred bond angles and distances for E−S bonds within a confined supramolecular system. Furthermore, this series of cryptands exemplifies the dynamic nature of main group "metal"-ligand self-assembly through the synthesis, transmetalation, and solution behavior of the cryptands, including the surprising observation of a stable, asymmetric conformation of the E_2L_3 cryptands.

These self-assembled main group complexes are reminiscent of organic cyclophanes (or heterophanes), where an −S−E−S− group substitutes for a heteroatom or a −C−X−C− unit. Our As_2L_3 cryptands[11a,f,12] are structurally similar to bicyclophanes,[24,25] specifically the π-prismands, and our recently reported As_4L_2 complex[11j] is remarkably similar to tetrathia-[3.3.3.3]cyclophane.[26] However, our assemblies differ from their organic analogues by resulting from a self-assembly reaction rather than a stepwise synthesis, resulting in typically high yields. Additionally, organic prismands lack the conformational isomerism and transmetalation properties exhibited by the main group congeners. This new generation of metallacyclophanes and metallacycles could allow access to new structure types and dynamic host−guest interactions.[27]

Experimental Section

General Procedures. ^{1}H NMR spectra were measured using Varian INOVA-300 and 500 spectrometers, and ^{13}C and ^{31}P NMR spectra were collected on a Varian INOVA-500 spectrometer in $CDCl_3$. Spectra were referenced using the residual solvent resonances as internal standards and reported in ppm. Mass spectrometry data were collected by directly injecting a $CHCl_3$ solution of cryptand into the spray chamber. Single crystal X-ray diffraction studies were performed on a Bruker SMART APEX diffractometer. Commercially available reagents were used as received. The reported yields are for isolated crystals. ***Caution!*** *Arsenic and antimony compounds are highly toxic and should be handled with care*. (This accounts for the small scale of the reactions reported herein.) The preparation of 1,4-bis(mercaptomethyl)naphthalene (H_2L),[11d] P_2L_3 and As_2L_3 via transmetalation, and Sb_2L_3 and Bi_2L_3 were previously reported.[12]

$AsSbL_3$. $AsCl_3$ (8.16 μL, 95.6 μmol), $SbCl_3$ (21.8 mg, 95.6 μmol), and diisopropylethylamine (DIPEA) (474 μL, 2.87 mmol) were dissolved in $CHCl_3$ (50 mL) under N_2 at 50 °C. H_2L (70.0 mg, 320 μmol) was added, and the solution was stirred for 3 h. After cooling the reaction mixture to 25 °C, it was washed with H_2O (20 mL) and 2 M NaOH (20 mL) and dried with brine (20 mL) and $MgSO_4$. The solution was layered with CH_3CN resulting in clear, colorless needles after 24 h (7.22 mg, 8.09 μmol, 8% crystalline yield). The crystals were dissolved in $CDCl_3$, and the ^{1}H NMR spectrum revealed that the product is 87% $AsSbL_3\cdot CH_3CN$ and 13% $Sb_2L_3\cdot CH_3CN$. ^{1}H NMR (300 MHz, $CDCl_3$): δ 8.43 (m, 6H, C*H*), 7.68 (m, 6H, C*H*), 5.87 (AB*q*, 6H, C*H*, J = 7.0 Hz), 4.37 (d, 3H, CH_2, J = 13.0 Hz), 4.24 (d, 3H, CH_2, J = 13.0 Hz), 3.99 (d, 3H, CH_2, J = 13.0 Hz), 3.91 (d, 3H, CH_2, J = 13.0 Hz). ^{13}C{^{1}H} NMR (125 MHz, $CDCl_3$): δ = 136.3, 133.6, 132.0, 131.6, 126.43, 126.37, 126.35, 125.9, 125.2, 124.4, 33.8, 32.3 ppm. APCI-MS: [H{$AsSbL_3$}]$^+$ calcd 850.9, found 851.0.

$AsBiL_3$. $AsCl_3$ (11.8 μL, 138 μmol) and $BiCl_3$ (43.5 mg, 138 μmol) were dissolved in dry MeOH (10 mL) and tetrahydrofuran (THF, 40 mL) and placed under N_2. DIPEA (684 μL, 4.14 mmol) was added, followed by H_2L (94.9 mg, 430 μmol), and the solution was stirred at 25 °C overnight. $CHCl_3$ (30 mL) was added, then the mixture was washed with H_2O (20 mL) and 2 M NaOH (20 mL) and dried with brine (20 mL) and $MgSO_4$. The solution was concentrated in vacuo to yield a bright yellow solid which was suspended in $CHCl_3$ (10 mL), filtered, and layered with pentane to yield pale yellow needles of $AsBiL_3\cdot 2CHCl_3$ after a day (12 mg, 10.2 μmol, 7% crystalline yield). ^{1}H NMR (300 MHz, $CDCl_3$): δ 8.45 (m, 6H, C*H*), 7.68 (m, 6H, C*H*), 6.02 (d, 3H, C*H*, J = 7.0 Hz), 5.80 (d, 3H, C*H*, J = 7.0 Hz), 5.61 (d, 3H, CH_2, J = 12.3 Hz), 4.23 (d, 3H, CH_2, J = 12.8 Hz), 4.13 (d, 3H, CH_2, J = 12.3 Hz), 3.98 (d, 3H, CH_2, J = 12.8 Hz). ^{13}C{^{1}H} NMR (125 MHz, $CDCl_3$): δ = 139.1, 133.8, 132.2, 131.5, 126.7, 126.6, 126.5, 125.9, 125.3, 123.2, 33.9, 31.9 ppm. APCI-MS: [H{$AsBiL_3$}]$^+$ calcd 939.0, found 939.1.

$PSbL_3$. Clear, colorless X-ray quality needles of $PSbL_3\cdot CH_3CN$ were isolated from the previously reported[12] synthesis of P_2L_3 from $Sb_2L_3\cdot CH_3CN$ with PBr_3. These were dissolved in $CDCl_3$ for further analysis. ^{1}H NMR (500 MHz, $CDCl_3$): δ 8.43 (m, 6H, C*H*), 7.67 (m, 6H, C*H*), 5.94 (d, 3H, C*H*, J = 6.8 Hz), 5.70 (d, 3H, C*H*, J = 7.2 Hz), 4.37 (d, 3H, CH_2, J = 12.4 Hz), 4.17 (d, 1.5H, CH_2, J = 13.0 Hz), 4.15 (d, 1.5H, CH_2, J = 12.5 Hz), 3.96 (d, 1.5H, CH_2, J = 13.0 Hz), 3.95 (d, 1.5H, CH_2, J = 12.5 Hz), 3.93 (d, 3H, CH_2, J = 12.4 Hz). ^{31}P NMR (500 MHz, $CDCl_3$): δ 86.7 (s). ^{13}C{^{1}H} NMR (125 MHz, $CDCl_3$): δ = 136.1, 132.4, 132.2, 131.4, 126.4, 126.3, 126.2, 126.05, 125.8, 124.5, 34.38 (d, $^2J_{CP}$ = 9 Hz), 32.2 ppm. APCI-MS: [H{$SbPL_3$}]$^+$ calcd 807.0, found 807.0.

X-ray Crystallography. Diffraction intensities for $AsSbL_3$, $AsBiL_3$, and $SbPL_3$ were collected at 173(2) K on a Bruker Apex CCD diffractometer using MoKα radiation λ = 0.71073 Å. Space groups were determined based on systematic absences. Absorption corrections were applied by SADABS.[28] Structures were solved by direct methods and Fourier techniques and refined on F^2 using full matrix least-squares procedures. All non-H atoms were refined with anisotropic thermal parameters.

(13) (a) Tanya, K. R.; Jane, N.; Geoffrey, B. J.; John, C. J.; Sally, B. *Eur. J. Inorg. Chem.* **2004**, *2004*, 2570–2584. (b) Lindsay, H. U.; Jean-Paul, G.; Nathalie, K.; Kalle, N.; Kari, R.; Jean-Marie, L. *Chem.—Eur. J.* **2005**, *11*, 2549–2565. (c) Cari, D. P.; Kelly, S. C.; Andrea, J. P.; Gareth, W. V. C.; Stuart, J. C.; Stoddart, J. F. *Angew. Chem., Int. Ed.* **2007**, *46*, 218–222.
(14) Riis-Johannessen, T.; Bernardinelli, G.; Filinchuk, Y.; Clifford, S.; Favera, N. D.; Piguet, C. *Inorg. Chem.* **2009**, *48*, 5512–5525.
(15) Akine, S.; Taniguchi, T.; Nabeshima, T. *Angew. Chem., Int. Ed.* **2002**, *41*, 4670–4673.
(16) Albrecht, M.; Liu, Y. F.; Zhu, S. C. S.; Schalley, C. A.; Frohlich, R. *Chem. Commun.* **2009**, 1195–1197.
(17) Andruh, M. *Chem. Commun.* **2007**, 2565–2577 and references therein.
(18) Petitjean, A.; Kyritsakas, N.; Lehn, J.-M. *Chem.—Eur. J.* **2005**, *11*, 6818–6828.
(19) Dietrich-Buchecker, C.; Colasson, B.; Fujita, M.; Hori, A.; Geum, N.; Sakamoto, S.; Yamaguchi, K.; Sauvage, J.-P. *J. Am. Chem. Soc.* **2003**, *125*, 5717–5725.
(20) Piguet, C.; Hopfgartner, G.; Bocquet, B.; Schaad, O.; Williams, A. F. *J. Am. Chem. Soc.* **1994**, *116*, 9092–9102.
(21) Hahn, F. E.; Offermann, M.; Schulze Isfort, C.; Pape, T.; Fröhlich, R. *Angew. Chem., Int. Ed.* **2008**, *47*, 6794–6797.
(22) (a) Funeriu, D. P.; Lehn, J.-M.; Fromm, K. M.; Fenske, D. *Chem.—Eur. J.* **2000**, *6*, 2103–2111. (b) Stulz, E.; Scott, S. M.; Bond, A. D.; Teat, S. J.; Sanders, J. K. M. *Chem.—Eur. J.* **2003**, *9*, 6039–6048.
(23) Piguet, C.; Bernardinelli, G.; Williams, A. F.; Bocquet, B. *Angew. Chem., Int. Ed. Engl.* **1995**, *34*, 582–584.
(24) Kunze, A.; Bethke, S.; Gleiter, R.; Rominger, F. *Org. Lett.* **2000**, *2*, 609–612.
(25) Kunze, A.; Gleiter, R.; Rominger, F. *Chem. Commun.* **1999**, 171–172.
(26) Klieser, B.; Vögtle, F. *Angew. Chem., Int. Ed. Engl.* **1982**, *21*, 618.
(27) Vögtle, F.; Pawlitzki, G.; Hahn, U. In *Modern Cyclophane Chemistry*; Gleiter, R., Hopf, H., Eds.; Wiley-VCH: Weinheim, 2004; pp 41−80.
(28) Sheldrick, G. M. *SADABS, Bruker/Siemens Area Detector Absorption Correction Program*; Bruker AXS: Madison, WI, 1998.

All H atoms in AsSb**L**$_3$ and AsBi**L**$_3$ were refined in calculated positions in a rigid group model. H atoms in Sb**P**$\mathbf{L}_3$ were found from the F-map and refined with isotropic thermal parameters. In the crystal structures of AsSb**L**$_3$ and Sb**P**$\mathbf{L}_3$ there were solvent molecules, CH_3CN, disordered over two positions related by a mirror plane. These molecules were isolated in the crystal packing and were not involved in specific interactions with the cryptand molecules. These disordered molecules were treated by SQUEEZE.[29] Corrections of the X-ray data by SQUEEZE (42 and 44 electron/cell, respectively for AsSb**L**$_3$ and Sb**P**$\mathbf{L}_3$) were close to the required values of 44 electrons/cell for two molecules in the full unit cells. In the crystal structure of AsBi**L**$_3$ there were two solvent $CHCl_3$ molecules. One of these molecules was disordered over two positions related by a mirror plane. The disordered $CHCl_3$ molecule was refined with restrictions; the value of 1.75 Å was used as a target for the C−Cl distances in the refinement. H atoms in the disordered solvent molecules were not taken into consideration. In the structures of AsSb**L**$_3$ and Sb**P**$\mathbf{L}_3$ the Sb/As and Sb/P atoms, respectively, shared two positions related by a mirror plane. The refinement of occupation factors provided a ratio for these atoms: $As_{0.92}Sb_{1.08}$ in AsSb**L**$_3$ and $Sb_{1.01}P_{0.99}$ in Sb**P**$\mathbf{L}_3$. In the structure of AsBi**L**$_3$, the Bi and As atoms disordered over two symmetrically independent positions. The refinement occupation factors for a model in which the Bi and As atoms shared these two positions provided a ratio for the Bi/As atoms of 0.565/0.435 and 0.417/0.583, respectively for the two positions, and the total ratio was $As_{1.02}Bi_{0.98}$. All calculations were performed by the Bruker SHELXTL (v. 6.10) package.[30]

Crystallographic Data for AsSb$\mathbf{L}_3\cdot CH_3CN$. $C_{38}H_{33}As_{0.92}NS_6Sb_{1.08}$, $M = 896.66$, $0.42 \times 0.08 \times 0.07$ mm, $T = 173(2)$ K, hexagonal, space group $P6_3/m$, $a = b = 11.4342(7)$ Å, $c = 16.131(2)$ Å, $V = 1826.5(3)$ Å^3, $Z = 2$, $D_c = 1.630$ Mg/m^3, $\mu = 2.012$ mm^{-1}, $F(000) = 899$, $2\theta_{max} = 54.00°$, 18014 reflections, 1387 independent reflections [$R_{int} = 0.0574$], $R_1 = 0.0318$, $wR_2 = 0.0722$ and GOF = 1.108 for 1387 reflections (69 parameters) with $I > 2\sigma(I)$, $R_1 = 0.0399$, $wR_2 = 0.0761$, and GOF = 1.108 for all reflections, max/min residual electron density +0.520/−0.226 e Å^3.

Crystallographic Data for AsBi$\mathbf{L}_3\cdot 2(CHCl_3)$. $C_{38}H_{32}As_{1.02}Bi_{0.98}Cl_6S_6$, $M = 1177.60$, $0.17 \times 0.14 \times 0.09$ mm, $T = 173(2)$ K cubic, space group $P2_13$, $a = b = c = 16.4744(8)$ Å, $V = 4471.2(4)$ Å^3, $Z = 4$, $D_c = 1.749$ Mg/m^3, $\mu = 5.344$ mm^{-1}, $F(000) = 2296$, $2\theta_{max} = 54.00°$, 9348 reflections, 3177 independent reflections [$R_{int} = 0.0553$], the Flack parameter is 0.037(11), $R_1 = 0.0449$, $wR_2 = 0.1023$, and GOF = 1.016 for 3177 reflections (164 parameters) with $I > 2\sigma(I)$, $R_1 = 0.0530$, $wR_2 = 0.1053$, and GOF = 1.026 for all reflections, max/min residual electron density +01.089/−0.619 e Å^3.

Crystallographic Data for Sb$\mathbf{P}\mathbf{L}_3\cdot CH_3CN$. $C_{38}H_{33}NPS_6Sb$, $M = 848.73$, $0.32 \times 0.10 \times 0.09$ mm, $T = 173(2)$ K, hexagonal, space group $P6_3/m$, $a = b = 11.3830(6)$ Å, $c = 16.1453(18)$ Å, $V = 1811.7(2)$ Å^3, $Z = 2$, $D_c = 1.556$ Mg/m^3, $\mu = 1.181$ mm^{-1}, $F(000) = 860$, $2\theta_{max} = 54.00°$, 10291 reflections, 1382 independent reflections [$R_{int} = 0.0319$], $R_1 = 0.0334$, $wR_2 = 0.0810$, and GOF = 1.114 for 1382 reflections (89 parameters) with $I > 2\sigma(I)$, $R_1 = 0.0405$, $wR_2 = 0.0849$, and GOF = 1.114 for all reflections, max/min residual electron density +0.726/−0.211 e Å^3.

Results and Discussion

Symmetric and Asymmetric $\mathbf{E_2L_3}$ Cryptands. Previously, our laboratory reported a series of E_2**L**$_3$ cryptands (where E = P, As, Sb, Bi) that were prepared by self-assembly reactions (Scheme 1).[12] When H_2**L** was mixed with $AsCl_3$, $SbCl_3$, or $BiCl_3$ in chloroform and the HCl byproduct was removed with base, E_2**L**$_3$ was formed. Sb_2**L**$_3$ and Bi_2**L**$_3$ were prepared in the presence of excess DIPEA, while As_2**L**$_3$ was prepared in the presence of KOH. A transmetalation[31] reaction could also be used to prepare As_2**L**$_3$, and "transmetallation" was the only effective route to form P_2**L**$_3$ (Scheme 2). Transmetalation occurred when Sb_2**L**$_3$ was treated with $AsCl_3$ or PBr_3 and As_2**L**$_3$ or P_2**L**$_3$ formed, respectively. For $Sb_2\mathbf{L}_3 \rightarrow As_2\mathbf{L}_3$, the reaction was shown to be quantitative by ^{1}H NMR spectroscopy.

Scheme 1. Self-Assembly of E_2**L**$_3$ Cryptands[a]

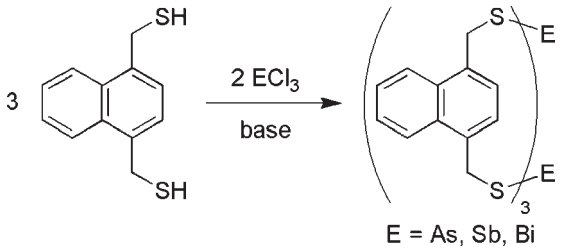

[a] DIPEA was used as the base for E = Sb or Bi, while KOH was used for E = As.

Scheme 2. Transmetallation of Sb_2**L**$_3$

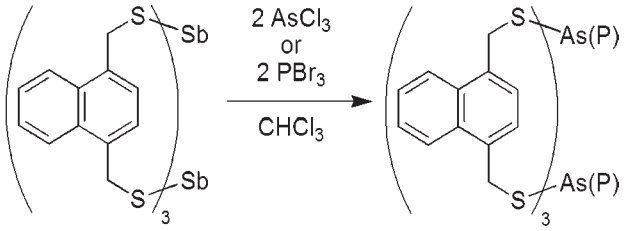

Solid-State Structures. We previously communicated the supramolecular transmetalation reaction that allowed for the synthesis of these cryptands, and this full paper provides a thorough structural analysis (solid-state and solution) of these systems in the context of three additional new heterometallic assemblies described in subsequent sections. Additionally, this paper describes a surprising conformational isomerism for these cryptands in solution. X-ray quality crystals of the complexes were grown by the slow diffusion of acetonitrile (P_2**L**$_3$, Sb_2**L**$_3$, and Bi_2**L**$_3$) or pentane (As_2**L**$_3$) into a chloroform solution of cryptand. The structures for these symmetric cryptands are remarkably similar (Figure 1); the only significant differences are in the position of the pnictogen atoms, the E−S bond distances, and S−E−S bond angles (Table 1). With increasing atomic mass comes an increase in E−S bond length and a decrease in the E···E distance. These differences are compensated for by the decreasing S−E−S angle, allowing the ligands to maintain almost identical positions in each cryptand (Figure 2). This trend is expected as the extent of s-character in the E−S bonds decreases going down the group. A search of the Cambridge Structural Database (CSD) for pnictogens bonded to three sulfur atoms in unconstrained systems reveals that this supramolecular coordination does not greatly

(29) Van der Sluis, P.; Spek, A. L. *Acta Crystallogr., Sect. A* **1990**, *A46*, 194–201.

(30) *SHELXTL, Program for Structure Solution, Refinement and Presentation*, 6.10; BRUKER AXS Inc.: Madison, WI.

(31) Transmetalation is used to describe the replacement of one Group 15 element with another, even when the replacement is not a metal as in the case of As (metalloid) and P (non-metal). This language is consistent with our previous communication on the topic (ref 12).

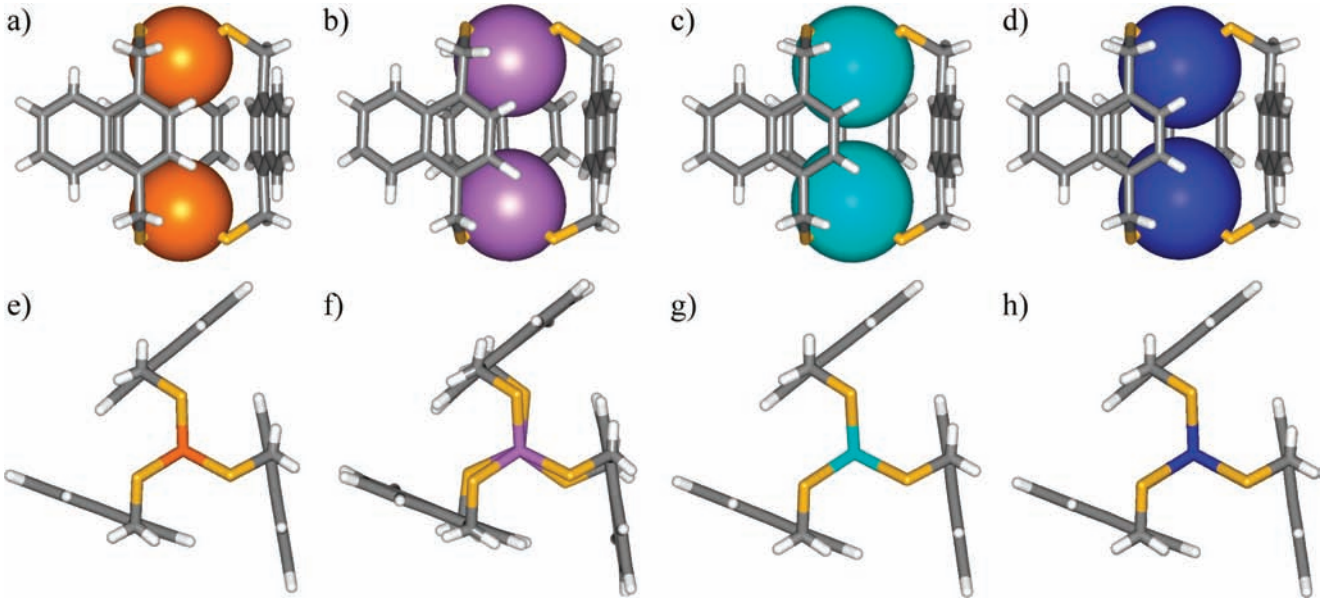

Figure 1. Stick and space-filling representations of the X-ray crystal structures of symmetric cryptands (a, e) $P_2\mathbf{L}_3$, (b, f) $As_2\mathbf{L}_3$, (c, g) $Sb_2\mathbf{L}_3$, and (d, h) $Bi_2\mathbf{L}_3$. Phosphorus is shown in orange, arsenic in purple, antimony in teal, bismuth in blue, sulfur in yellow, carbon in gray, and hydrogen in white.

Table 1. Select Distances and Bond Angles for $E_2\mathbf{L}_3$ Cryptands

	$P_2\mathbf{L}_3$	$As_2\mathbf{L}_3$	$Sb_2\mathbf{L}_3$	$Bi_2\mathbf{L}_3$
E···E (Å)	5.491	5.108	4.827	4.683
E−S (Å)	2.1182(12)	2.2514(10)	2.4206(5)	2.5157(10)
CSD average E−S (Å)	2.144	2.298	2.470	2.592
S−E−S (deg)	96.52(5)	94.00(4)	91.456(18)	90.84(3)
CSD average S−E−S (deg)	95.24	91.35	91.09	90.71
E···C_{aryl} (Å)	3.251 3.544	3.300 3.577	3.343 3.584	3.358 3.548

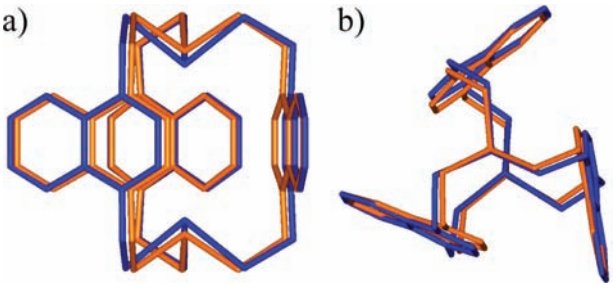

Figure 2. Overlayed stick-representations of the X-ray crystal structures of the symmetric cryptands $P_2\mathbf{L}_3$ (orange) and $Bi_2\mathbf{L}_3$ (blue) from side (a) and top-down (b) views.

affect the bonding geometry of the pnictogens. In each of the $E_2\mathbf{L}_3$ structures, the E−S distance is slightly shorter than, but within 0.1 Å of, the CSD average. The S−E−S bond angles in the $E_2\mathbf{L}_3$ structures are slightly larger than the CSD average, but within a couple degrees (and not out of the normal range).

Six η^2 E···π interactions stabilize each of the $As_2\mathbf{L}_3$, $Sb_2\mathbf{L}_3$, and $Bi_2\mathbf{L}_3$ cryptands. The E···π interaction is an attractive interaction involving dispersion forces and the donation of π-electrons from the aryl ring into a σ^* orbital

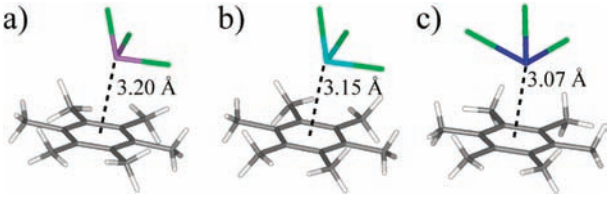

Figure 3. Stick representations of crystal structures of (a) $AsCl_3$,[36] (b) $SbCl_3$,[37] and (c) $BiCl_3$[38] cocrystallized with hexamethylbenzene, reported by Schmidbaur and co-workers. The dashed lines represent the short E···π interactions (distances to ring centroids are shown in each case).

on E.[32−34] In $P_2\mathbf{L}_3$, the six shortest P···C_{aryl} contacts are also shorter than the sum of the van der Waals radii (3.5 Å), but no attractive P···π interactions are known or expected.[35] Each symmetric $E_2\mathbf{L}_3$ cryptand possesses crystallographic C_{3h} symmetry, except $As_2\mathbf{L}_3$, which is slightly offset and has C_3 crystallographic symmetry. This could be a result of the As···π interactions causing the ligands to twist more to allow the metals to sit deeper within the cavity or it could be a consequence of crystal packing. The E···π interaction is known to be stronger for the larger pnictogens, typically resulting in a *decrease* in the E···C_{aryl} distance (Figure 3).[34] However, the opposite trend is observed here. In these supramolecular cryptands, the shortest E···C_{aryl} distance *increases* from $As_2\mathbf{L}_3$ to $Sb_2\mathbf{L}_3$ to $Bi_2\mathbf{L}_3$. This is not an indication of a weaker E···π interaction, but is likely due to the growing radius of E, the consequently longer E−S bonds, and the constricted position of the metals within the cryptand cavity.

(32) Schmidbaur, H.; Schier, A. *Organometallics* **2008**, *27*, 2361–2395 and references therein.

(33) Auer, A. A.; Mansfeld, D.; Nolde, C.; Schneider, W.; Schurmann, M.; Mehring, M. *Organometallics* **2009**, *28*, 5405–5411.

(34) Cangelosi, V. M.; Pitt, M. A.; Vickaryous, W. J.; Allen, C. A.; Zakharov, L. N.; Johnson, D. W. *Cryst. Growth Des.* **2010**, *10*, 3531−3536.

(35) η^6-arene complexation to phosphenium cations is known, but very rare. See: Burford, N.; Clyburne, J. A. C.; Bakshi, P. K.; Cameron, T. S. *J. Am. Chem. Soc.* **1993**, *115*, 8829–8830. The Cambridge Structural Database was searched for P···π contacts of less than the sum of the van der Waals radii for P and C, turning up 20 hits. However, no correlation between contact distance and angle was observed. See Supporting Information for further detail.

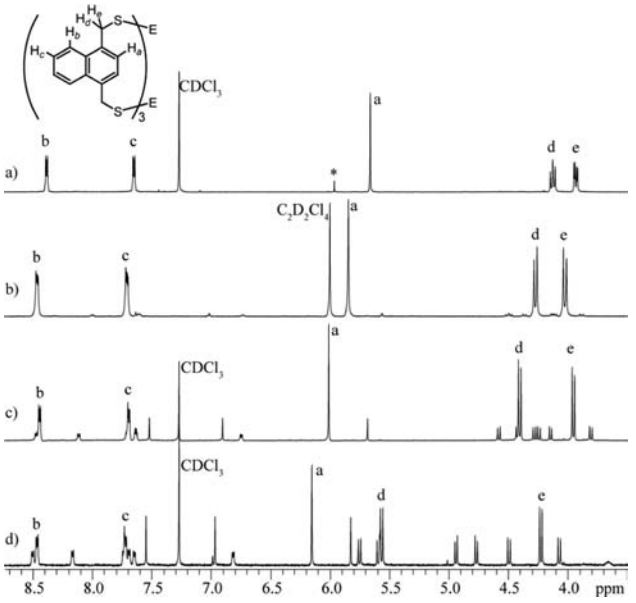

Figure 4. ^{1}H NMR spectra for (a) $P_2\mathbf{L}_3$, (b) $As_2\mathbf{L}_3$, (c) $Sb_2\mathbf{L}_3$, and (d) $Bi_2\mathbf{L}_3$. The signals from the symmetric cryptands are labeled, while those for the asymmetric cryptands are unlabeled (See Supporting Information for complete labeling scheme). * denotes $C_2H_2Cl_4$ in the spectrum.

Solution Structures. In solution each of the $E_2\mathbf{L}_3$ cryptands is present in two different conformations. The first is a symmetric conformer similar to that in the solid state, in which each of the three ligands are equivalent and the complex has overall C_{3h} symmetry. Figure 4 shows the ^{1}H NMR spectra for each of the cryptands. The exterior aryl protons H_b and H_c are in very similar positions in each cryptand and are not affected by the identity of E, as shown by the almost identical resonance shifts for each cryptand. The resonance for interior proton H_a differs slightly depending on the pnictogen, shifting downfield from $P_2\mathbf{L}_3$ to $Bi_2\mathbf{L}_3$. The methylene protons, H_d and H_e, are more significantly affected by the identity of E. In $P_2\mathbf{L}_3$, the resonance for each of these protons is split into a doublet of doublets because of splitting by the other methylene proton and the nearby phosphorus nucleus. In each of $As_2\mathbf{L}_3$, $Sb_2\mathbf{L}_3$, and $Bi_2\mathbf{L}_3$, these methylene resonances appear as a single pair of doublets with chemical shifts based on the identity of E. Similarly to proton H_a, the signals for H_d and H_e in $Bi_2\mathbf{L}_3$ are shifted the farthest downfield.

A glaring feature of the ^{1}H NMR spectra of $Sb_2\mathbf{L}_3$ and $Bi_2\mathbf{L}_3$ is the presence of a second, less-symmetric species in solution. Careful analysis also reveals a second species in the spectrum for $As_2\mathbf{L}_3$, but not in that for $P_2\mathbf{L}_3$. Each NMR sample was prepared by dissolving crystals of symmetric cryptand and, initially, only the symmetric cryptand was observed. However, over the course of half of an hour a conformational change established a new equilibrium between the symmetric $E_2\mathbf{L}_3$ cryptand and an asymmetric species, $E_2\mathbf{L}_3$-*asym* (when E = As, Sb, or Bi). *g*COSY and NOESY NMR (Supporting Information, Figures S2−S9) were used to identify this asymmetric species as a cryptand in which one ligand has "flipped" (Figure 5a), perturbing the C_3 symmetry of the complex and resulting in a conformation with only C_s symmetry. While less than 5% of the $As_2\mathbf{L}_3$ cryptand is in this asymmetric form, it comprises 47% of the $Sb_2\mathbf{L}_3$ and 60% of the $Bi_2\mathbf{L}_3$ samples based on ^{1}H NMR integrals. To confirm that the observed species was not actually a higher order assembly, liquid chromatography mass spectrometry was carried out on a sample of $Sb_2\mathbf{L}_3$. As expected, two species with different retention times, yet the same mass-to-charge ratio, were present in solution (Supporting Information, Figure S12). The relative amount of each did not match the ratio observed by ^{1}H NMR spectroscopy, but that could be a result of solvent effects or conformational change occurring over the course of the experiment.

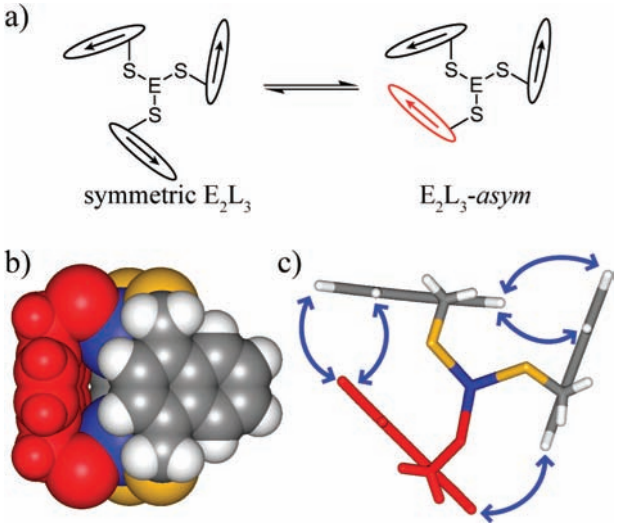

Figure 5. Cartoon representations of (a) symmetric $E_2\mathbf{L}_3$ (left) and $E_2\mathbf{L}_3$-*asym* (right) in which the ligands are represented by arrows. In the symmetric cryptand all of the ligands point counterclockwise. In the asymmetric cryptand, two ligands point counterclockwise (black) and the one "flipped" ligand points clockwise (red). The DFT-calculated structure of $Bi_2\mathbf{L}_3$-*asym* in (b) space-filling and (c) stick representations. The "flipped" ligand is shown in red. The blue arrows indicate the protons that were correlated by their NOEs in solution (Supporting Information, Figures S2−S9).

DFT calculations were carried out to help visualize the likely structure of $E_2\mathbf{L}_3$-*asym*. First, to judge the ability of the chosen DFT method (with a 6-31+G* basis set for all atoms and with the B3LYP functional),[11f,39] the structures of the symmetric $P_2\mathbf{L}_3$, $As_2\mathbf{L}_3$, $Sb_2\mathbf{L}_3$, and $Bi_2\mathbf{L}_3$ cryptands were calculated. These were found to match the crystal structures very closely (see overlays in Supporting Information, Figure S10). The only minor difference is that in the DFT-calculated structures, the metals and ligands were not pulled quite as tightly into the cavity. However, it has been established that this functional is not well suited for describing the E$\cdots\pi$ interaction,[11f] which is likely a general limitation of DFT since dispersion forces account for at least some of this attractive interaction.[33,34] However, we have found DFT to be very useful in qualitatively predicting the overall structures of Group 15-containing assemblies.[11f]

(36) Schmidbaur, H.; Nowak, R.; Steigelmann, O.; Muller, G. *Chem. Ber.* **1990**, *123*, 1221–1226.
(37) Schmidbaur, H.; Nowak, R.; Schier, A.; Wallis, J. M.; Huber, B.; Muller, G. *Chem. Ber.* **1987**, *120*, 1829–1835.
(38) Schier, A.; Wallis, J. M.; Muller, G.; Schmidbaur, H. *Angew. Chem., Int. Ed. Engl.* **1986**, *25*, 757–759.
(39) Models were minimized using Spartan '08 (Wave function, Inc., 182 Irvine, CA, 2008). The choice of functional and basis sets was based on those used in ref 40.

The structures of P_2L_3-*asym*, As_2L_3-*asym*, Sb_2L_3-*asym*, and Bi_2L_3-*asym* were determined, and it was found that in each case a stable structure was converged upon in which one ligand has "flipped" (Figure 5b,c for Bi_2L_3-*asym*, Supporting Information, Figure S11). These DFT calculations revealed that each of the symmetric cryptands was more stable than each of the asymmetric cryptands by 4−6 kcal/mol (6.6 for P_2L_3, 5.3 for As_2L_3, 4.0 for Sb_2L_3, and 4.0 for Bi_2L_3) (Supporting Information, Table S2). These energy differences are much larger than those observed by ^{1}H NMR spectroscopy, likely because of solvation effects and a limitation of DFT in predicting E···π interactions, but the general trend fits: the energy difference is smaller for the heavier pnictogens. However, these calculations do not show that Bi_2L_3-*asym* is lower in energy than its symmetric counterpart even though we observe that it is 0.24 kcal/mol lower by ^{1}H NMR spectroscopy (energy differences calculated by measuring the ratio of conformers at equilibrium).

It is not immediately clear why the asymmetric cryptands are relatively more stable when compared to their symmetric counterparts for the heavier pnictogens. The simplest possible explanation is that it is a steric effect of the larger elements.[40] The larger pnictogens require more space within the cavity, and the "flipping" of one ligand provides that accommodation. The average of the six shortest E···C_{aryl} contacts in the DFT calculated model of Sb_2L_3-*asym* (3.53 Å) was found to be slightly longer than that for the crystal structure of Sb_2L_3 (3.46 Å), suggesting that the "flipping" does indeed open up more space. While we cannot confirm the accuracy of the models without a crystal structure of the asymmetric cryptand (which remains elusive), we can compare them to what is observed in solution. ^{1}H NMR spectroscopy shows that the proton resonances for Bi_2L_3-*asym* and Sb_2L_3-*asym* follow the same pattern but are significantly shifted based on proximity to the pnictogens. The similarity of these structures is corroborated by overlaying the DFT-calculated structures (Supporting Information, Figure S15).

Another possible explanation for the trend in the relative stability of the two conformations of cryptand is that the asymmetric conformation may allow for stronger E···π interactions, and the strength of the E···π interaction increases down the group (Figure 3) (this would also explain the poor prediction of the conformational energy differences by DFT). Consequently, Bi_2L_3-*asym* is stabilized more than Sb_2L_3-*asym* and As_2L_3-*asym* compared to their symmetric counterparts. In the symmetric cryptands, each pnictogen atom is involved in three E···π interactions, as evidenced by the short E···C_{aryl} contacts observed in the crystal structures. Although the shortest calculated E···C_{aryl} contacts for the "flipped" ligand are not as short as they are within the symmetric cryptand, the position of the ligand is thought to result in a stronger E···π interaction. In the model, the "flipped" ligand is positioned such that it is sitting deep into the cryptand cavity with *three* carbon atoms close to the pnictogen (within the sum of the van der Waals radii) allowing for an η^3-interaction (as compared to the η^2-interaction observed in the symmetric cryptand). Additionally, the calculated S−E···C_{aryl} angle is larger in the asymmetric cryptands. This angle is 160° for Sb_2L_3-*asym* and 155° in the symmetric cryptand. The larger angle allowed by the flipping of the ligand may result in a stronger Sb···π interaction, although our laboratory has previously published a structural survey that shows that the average angle for non-constrained interactions is 155° for Sb.[34] While we previously noted that DFT does not describe E···C_{aryl} contacts well, the position of this ligand deep within the cryptand can also be observed in solution (as evidenced by the upfield-shifted resonance for H_c on this ligand (~6.8 ppm)).

Mechanism of Ligand Flipping. Semiempirical AM1 calculations were carried out to see if it was energetically feasible for a ligand to "flip" without breaking any bonds. On the basis of these calculations and a visual examination of the space-filling models, it is clear that this is not the route to interconversion between E_2L_3 and E_2L_3-*asym*. The cavity is far too sterically congested to allow even the short end of a naphthalene ring to pass through it. Rather, it is far more likely that the mechanism to interconversion is through the breaking and reforming of an E−S bond. While that bond is broken, the ligand can rotate freely without steric considerations. The strength of an As−S bond is estimated to be ~81 kcal/mol;[41] nonetheless, these bonds are labile enough to allow for ligand exchange,[42] self-assembly,[11h] and transmetalation.[12]

Heterometallic EE′L_3 Cryptands. Further synthesis was carried out to determine whether or not heterometallic cryptands could be prepared despite H_2L possessing only one type of coordination site. To test this possibility, H_2L was treated with $AsCl_3$, DIPEA, and either $SbCl_3$ or $BiCl_3$. Surprisingly, rather than all homometallic cryptands or a statistical mixture of cryptands, NMR spectroscopy on the crude reaction mixtures revealed that the heterometallic $AsSbL_3$ and $AsBiL_3$ cryptands were the dominant products of the reactions (>80% in each case), with the remainder of the product being homometallic cryptand. A heterometallic $PSbL_3$ cryptand was also prepared, but was isolated from a transmetalation reaction involving the treatment of Sb_2L_3 with PBr_3 that did not go to completion.

X-ray quality crystals of each of $AsSbL_3$, $AsBiL_3$, and $PSbL_3$ were grown by layering a chloroform solution of the complex with acetonitrile or pentane (Figure 6). Within each crystal, E and E′ are disordered to some degree over both positions, so all of the E···E′, E−S, and S−E-(E′)−S distances and angles are averaged for the two pnictogens (Table 2). Still, the averaged distances and angles fit into the trend observed in the homometallic E_2L_3 complexes. In each case, the E···E′ and E−S distances and S−E(E′)−S angles fall between the values for the two homometallic complexes, but are closer to what is observed for the heavier E_2L_3 complex. This suggests that the larger metals have more of an effect on the geometry than the smaller metals. Like their homometallic analogues, each of

(40) The van der Waals radii are 1.8 Å for P, 1.85 Å for As, 2.0 Å for Sb, and 2.0 Å for Bi. Taken from: Bondi, A. *J. Phys. Chem.* **1964**, *68*, 441–451.

(41) Bond strength approximated from As−S bond strengths in As_xS_y polyhedra: Babíc, D.; Rabii, S.; Bernholc *J. Phys. Rev. B: Condens. Matter Mater. Phys.* **1989**, *39*, 10831–10838.

(42) (a) Delnomdedieu, M.; Basti, M. M.; Otvos, J. D.; Thomas, D. J. *Chem.-Biol. Interact* **1994**, *90*, 139–155. (b) Delnomdedieu, M.; Basti, M. M.; Otvos, J. D.; Thomas, D. J. *Chem. Res. Toxicol.* **1993**, *6*, 598–602.

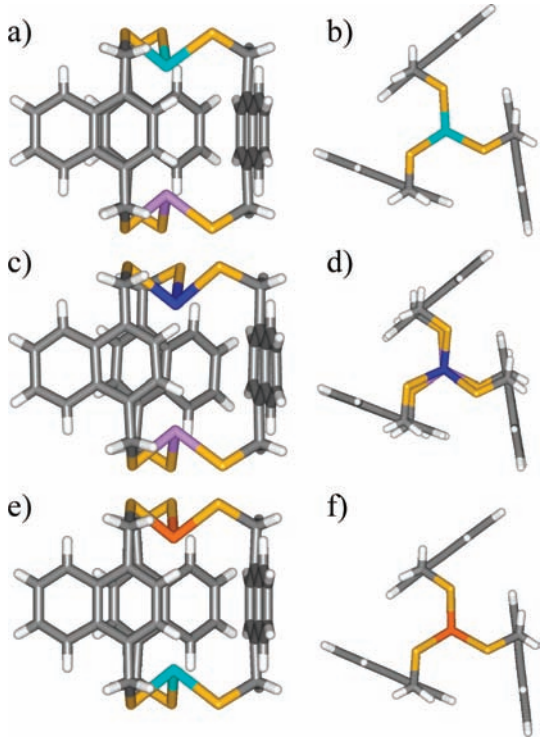

Figure 6. Stick representations of the X-ray crystal structures of (a, b) AsSb**L**$_3$, (c, d) AsBi**L**$_3$, and (e, f) PSb**L**$_3$. Phosphorus is shown in orange, arsenic in purple, antimony in teal, bismuth in blue, sulfur in yellow, carbon in gray, and hydrogen in white.

Table 2. Select Distances and Bond Angles for EE′**L**$_3$ Cryptands

	AsSb**L**$_3$	AsBi**L**$_3$	PSb**L**$_3$
E···E′ (Å)	4.944	4.685	4.960
E(E′)−S (Å)	2.3537(7)	2.4499(19) 2.376(2)	2.3212(7)
S−E(E′)−S (deg)	92.10(2)	89.96(7) 91.42(8)	91.26(2)
E(E′)···C$_{aryl}$ (Å)	3.302 3.553	3.278, 3.391 3.314, 3.570	3.263 3.524

the EE′**L**$_3$ cryptands exhibits six close E···C$_{aryl}$ contacts in the solid state, suggesting stabilization of the cryptands through E···π interactions.

In solution, the EE′**L**$_3$ cryptands are C_3-symmetric, just as they are in the solid state (Figure 7). Unlike their homometallic counterparts, no asymmetric cryptand is observed. This could be a result of ligand strain caused by the size difference in the metals, or there could be too little asymmetric cryptand to observe by NMR spectroscopy. Because of the lack of σ_h-symmetry in the complex, the splitting for the asymmetric (and chiral) heterometallic cryptand would be quite complex and at a low concentration they might not be observed in the spectra. For the symmetric heterometallic cryptand, the ^{1}H NMR resonances for H$_b$ and H$_{b'}$ and H$_c$ and H$_{c'}$ are relatively unchanged from their homometallic analogues, but the resonance for H$_a$ and H$_{a'}$ is split into an AB_q. This is due to the lack of σ_h symmetry in the heterometallic cryptands, making H$_a$ and H$_{a'}$ inequivalent. Additionally, the methylene protons at each end of the cryptand appear as separate sets of doublets (or two doublets of doublets for the P end of PSb**L**$_3$). Each of these resonances is shifted only slightly from where

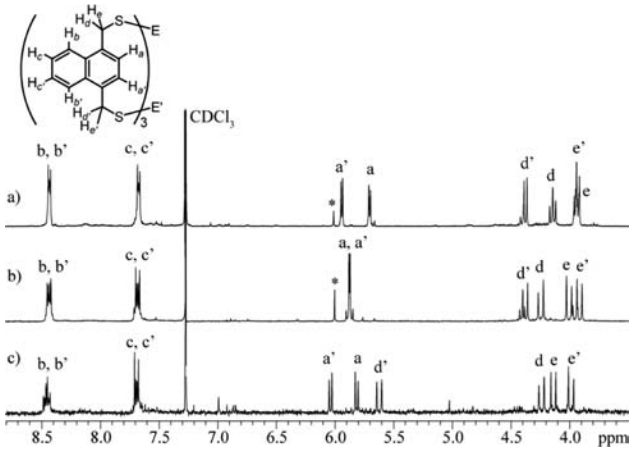

Figure 7. ^{1}H NMR spectra of EE′**L**$_3$ heterometallic cryptands: (a) PSb**L**$_3$, (b) AsSb**L**$_3$, and (c) AsBi**L**$_3$. * denotes Sb$_2$**L**$_3$ cryptand impurity.

they appear for the homometallic complexes suggesting that in solution, as in the solid state, the geometries around the metals are very similar to what they are for the homometallic complexes.

The heterometallic EE′**L**$_3$ cryptands are chiral, because of a right-handed or left-handed twist of the ligands around the chirality axis of the two metals. This chirality is different from that in most supramolecular helicates, where both (identical) metals experience the same handedness of the ligands connecting them.[43] Here, the metals experience different handedness, but if the two metals were swapped, one would be left with the enantiomer of the original molecule. While spontaneous resolution of one enantiomer was not obtained upon crystallization, it may be possible to separate the enantiomers on a chiral HPLC column. These cryptands are too small to fit guest molecules, but larger P-containing cryptands may be able to serve as host molecules with potential applications in chiral catalysis. We are exploring their use as a new class of trans-directing phosphine ligands.

Conclusion

A series of homometallic (P$_2$**L**$_3$, As$_2$**L**$_3$, Sb$_2$**L**$_3$, Bi$_2$**L**$_3$) and heterometallic (PSb**L**$_3$, AsSb**L**$_3$, AsBi**L**$_3$) cryptands were prepared directly from H$_2$**L** and ECl$_3$ or by transmetalation of Sb$_2$**L**$_3$, showing that P, As, Sb, and Bi can be used almost interchangeably in "metal"-directed self-assembly. Within this supramolecular framework, the geometries of P, As, Sb, and Bi with thiolate ligands can be directly compared, giving insight into the bonding preferences of these pnictogens. As expected, the E−S bonds lengthen and the S−E−S bond angles contract down the group. Surprisingly, in solution the homometallic C_{3h}-symmetric E$_2$**L**$_3$ cryptands rearrange into asymmetric conformers (E$_2$**L**$_3$-*asym*). Heterometallic cryptands were prepared including PSb**L**$_3$, which is a rare example of a chiral trans-directing phosphine, and AsBi**L**$_3$, which is a rare example of a chiral bismuth compound with axial chirality at each pnictogen. This work exemplifies the utility of Group 15 elements as "metals" in metal-directed supramolecular self-assembly.

(43) Seeber, G. T., Bryan, E. F.; Raymond, K. N. In *Top. Curr. Chem.*; Springer: Berlin: Heidelberg, 2006; Vol. *265*, p 147−183.

Acknowledgment. We gratefully acknowledge funding from the National Science Foundation (CAREER award CHE-0545206). D.W.J. is a Cottrell Scholar of Research Corporation for Science Advancement. This material is based upon work supported by the U.S. Department of Education under Award No. P200A070436 (V.M.C.) and an NSF Integrative Graduate Education and Research Traineeship No. DGE-0549503 (T.G.C.). The purchase of the QToF Mass Spectrometer was made possible by a grant from the NSF (CHE-0639170).

Supporting Information Available: X-ray data in CIF format, CSD refcodes, 1D and 2D NMR spectra, LCMS data, X-ray and DFT structures. This material is available free of charge via the Internet at http://pubs.acs.org.